

## Stacked organic solar cells based on pentacene and C<sub>60</sub>

David Cheyns<sup>a,b,\*</sup>, Hans Gommans<sup>a</sup>, Mathieu Odijk<sup>a,1</sup>, Jef Poortmans<sup>a</sup>, Paul Heremans<sup>a,b</sup>

<sup>a</sup>IMEC vzw, Polymer and Molecular Electronics, Kapeldreef 75, B-3001 Leuven, Belgium

<sup>b</sup>ESAT, Katholieke Universiteit Leuven, Kasteelpark Arenberg 10, B-3001 Leuven, Belgium

Available online 14 December 2006

### Abstract

In order to improve photon harvesting, two small molecule organic solar cells are placed in series on top of each other. These stacked cells need an efficient recombination center in between both cells. In this study we test vacuum deposited metal layers as recombination centers with pentacene and buckminsterfullerene (C<sub>60</sub>) as donor and acceptor, respectively. S-shaped curves are visible in the *I*–*V* characteristics when using thin layers of aluminum, indicating a barrier for extraction inside the device. Thin metal layers of gold or silver result in an increased open-circuit voltage without the appearance of these S-shaped features.

© 2006 Elsevier B.V. All rights reserved.

**Keywords:** Planar heterojunction solar cells; Stacked solar cells; Fullerene; Tandem

### 1. Introduction

Since the first appearance of organic solar cells a gradual improvement has been observed toward higher efficiencies [1–4]. Traditionally, full organic solar cells are divided in two fields, solution processable solar cells based on conjugated polymers and vacuum evaporated solar cells based on small molecules. With both techniques efficiencies up to 4% or 5% are achieved [5–7]. One drawback of organic photoactive materials is their narrow absorption window compared to the solar cells based on inorganic semiconductors. A possible way to extend the spectral sensitivity over a broader wavelength region is stacking different solar cells on top of each other. This can be done by placing the two cells in parallel or in series. Solar cells connected in series on top of each other are known as stacked or tandem cells [8–10]. To make things clear, the definition “stacked solar cell” will be used if the two cells consist of the same material set, while “tandem solar cells” use two different material sets. Only real tandem solar cells

will extend the spectral sensitivity. Nevertheless, stacked solar cells are a first step toward tandem solar cells.

The challenge of making stacked or tandem cells is in finding an efficient recombination center in between the two subcells to ensure their efficient series connection. In this paper different materials are studied as recombination centers to interconnect subcells based on pentacene and fullerene (C<sub>60</sub>). In the past thin layers of silver [9] or gold [8,10] were successfully used in combination with CuPc and C<sub>60</sub>, but a comparison study was lacking. Pentacene combined with C<sub>60</sub> as active layer for organic solar cells has recently gained interest [11,12]. Both materials show a high transistor mobility [13,14], which is beneficial for solar cells. Furthermore, pentacene has a peak absorption around 670 nm which is close to the maximum of the AM1.5 solar spectrum.

In this report, we start by making single cells and look at the influence of PEDOT:PSS as an additional interface layer at the transparent contact. Possible explanations for differences in open-circuit voltage (*V*<sub>oc</sub>) and short-circuit current are presented. In a next step, stacked cells are studied. We present a simple model to explain the working principle of stacked cells. Finally, two cells are stacked on top of each other and different metal layers are used as recombination layer in between the two cells.

\*Corresponding author. IMEC vzw, Polymer and Molecular Electronics, Kapeldreef 75, B-3001 Leuven, Belgium.

E-mail address: [david.cheyns@imec.be](mailto:david.cheyns@imec.be) (D. Cheyns).

<sup>1</sup>Present address: University of Twente, BIOS Chair, P.O. Box 217, NL-7500 AE Enschede, The Netherlands.

## 2. Single cells

Before stacking two cells on top of each other, single cells are made as references. The structure of the single planar heterojunction devices is as follows: glass plates covered with ITO ( $\leq 20 \Omega/\square$ ) from Merck display technologies are patterned using a screen-printed resist followed by an etching technique. All substrates are subsequently cleaned with solvents and oxygen plasma treatment. Half of the substrates are covered with a 40 nm thick PEDOT:PSS layer (HC Starck). Further production and current/voltage characterization occur in a nitrogen filled glove box system directly connected to a vacuum system.  $C_{60}$ , pentacene and 2,9-dimethyl-4,7-diphenyl-1,10-phenanthroline (bathocuproine or BCP) are bought from Aldrich and further purified using vacuum thermal gradient sublimation. BCP is a known exciton blocking layer [15], and has been proven to increase the efficiency of organic solar cells [16]. The organic materials are evaporated onto the substrates in an ultra-high vacuum chamber ( $10^{-8}$ – $10^{-9}$  Torr). Different organic layers are deposited using thermal evaporation with evaporation speeds between 0.5 and 1.0 Å/s. A 70 nm thick aluminum layer is used as the capping electrode and is deposited in a separate UHV-chamber without exposing to air. The samples are measured under a xenon arc lamp with AM1.5 filters

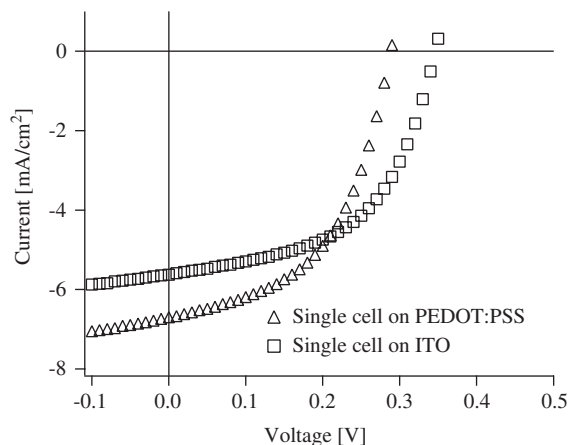


Fig. 1.  $I$ – $V$  curves of a single cell. Substrate:  $\square$ : glass/100 nm ITO,  $\triangle$ : glass/100 nm ITO/30 nm PEDOT:PSS. Subsequent layer structure: 40 nm pentacene/30 nm  $C_{60}$ /10 nm BCP/70 nm aluminum. The incident simulated AM1.5 light power is  $180 \text{ mW}/\text{cm}^2$ . The power conversion efficiencies for the cell with PEDOT: 0.55% ( $I_{sc} = 6.7 \text{ mA}/\text{cm}^2$ ,  $V_{oc} = 0.29 \text{ V}$ ,  $FF = 51\%$ ), without PEDOT: 0.58% ( $I_{sc} = 5.6 \text{ mA}/\text{cm}^2$ ,  $V_{oc} = 0.35 \text{ V}$ ,  $FF = 53\%$ ).

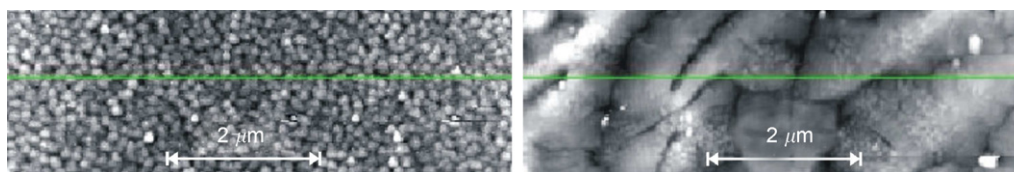


Fig. 2. AFM pictures of a 100 nm thick pentacene layer grown on ITO (left) and on PEDOT:PSS (right). Maximum height differences are 40 nm (left) and 30 nm (right).

(L.O.T. Oriel) with the light intensity being calibrated with a silicon detector. The voltage is applied and current is read out with a HP4156c parameter analyzer. The solar cell area is  $3 \text{ mm}^2$ .

Single cells with layer structure 100 nm ITO/(40 nm PEDOT:PSS/) 40 nm pentacene/30 nm  $C_{60}$ /10 nm BCP/70 nm aluminum are made. The measured  $I$ – $V$  characteristics for single cells with and without PEDOT:PSS on the ITO can be seen in Fig. 1. Cells with PEDOT:PSS have a higher short-circuit current but a lower open-circuit voltage compared to the cells without PEDOT:PSS. As a result the efficiencies are almost the same.

We discuss two possible explanations for the change in short-circuit current and open-circuit voltage. The first explanation we tentatively propose is the change in morphology of pentacene grown on ITO or on PEDOT:PSS. The two different substrates give different crystal growths for pentacene, as can be concluded from AFM pictures (Fig. 2). Different crystals can cause different mobilities, a change in donor–acceptor interface or/and a change in trap levels and as such change the solar cell characteristics.

Smaller features for pentacene grown on ITO can be seen on the AFM pictures of Fig. 2, compared to the big crystals for pentacene grown on PEDOT:PSS. This suggests a more folded interface area between pentacene and  $C_{60}$  for solar cells made on ITO. The pentacene crystals have a diameter of 200 nm and a height of 40 nm. With these dimension, possible gain of an increased interface area is not high (5–8% increase in exciton collection area expected).

Another explanation for the change in  $I$ – $V$  characteristics can be found by looking at the optical interference patterns inside the organic layers. Due to the small thicknesses of the layers back reflection at each interface causes peaks and valleys of the light intensity inside the film [17]. This optical interference is of great importance when optimizing devices: high optical fields should be located at the places where dissociation centers can be found [18,19]. Both reflection and absorption are important when looking at optical interference and both parameters are included in the complex index of refraction ( $n + ik$ ) [20]. The complex index of refraction of all materials used in this study are measured by ellipsometry (SOPRA, gesp5). The values measured for the organic materials can be seen in Fig. 3. As the  $k$ -value is proportional to the absorption coefficient ( $\alpha = 4\pi k/\lambda$ ), Fig. 3 shows the onset of absorption for pentacene at 700 nm.

An optical simulator is written in Matlab and uses the complex index of refraction values to calculate the optical field inside the different layers. The results of the optical simulation for the single pentacene/C<sub>60</sub> solar cells can be seen in Fig. 4. The figure shows the amount of absorbed photons as a function of the wavelength throughout the device structure when using normalized full-spectrum incident light. Only the organic layers are shown, a thick glass substrate, a 100 nm ITO layer underneath and a

70 nm aluminum layer on top are not shown but are included in the simulation. The amount of absorbed photons close to the pentacene-C<sub>60</sub> interface can be related to the short-circuit current. Integration over the thickness of the pentacene layer and over the wavelength range shown gives  $2.65 \times 10^{17}$  and  $3.35 \times 10^{17}$  absorbed photons for the cell made on ITO and PEDOT:PSS, respectively. This could give an indication for the higher current inside the cells with PEDOT:PSS.

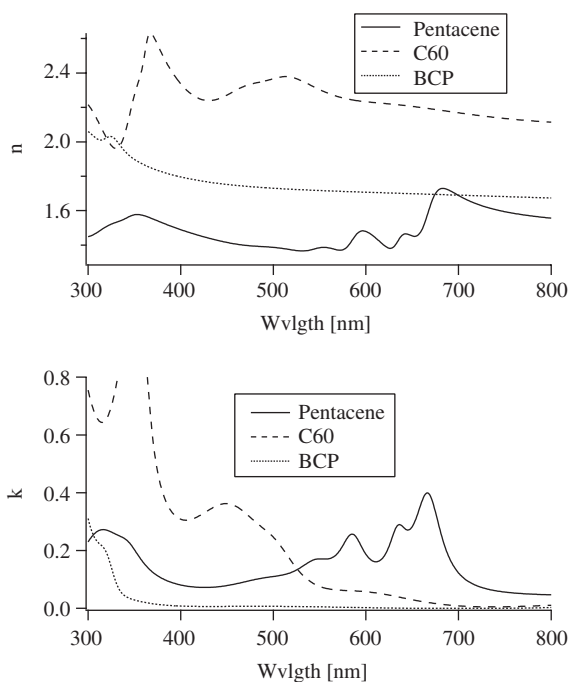


Fig. 3.  $n$ - and  $k$ -values of organic materials used in this paper.

### 3. Stacked cells

In stacked configuration, two subcells are combined in series with a recombination center in between. In this paper, by definition, the first cell is the cell closest to the incident light, the second cell is the cell closest to the top-contact. By Kichoff's law, a series configuration requires the same current flowing through the two subcells. If the amount of free carriers generated by one subcell is higher than the amount of the other cell, the surplus in carriers cannot flow to the outside circuit. Carriers will go to the recombination zone, where they wait for recombination with carriers of the opposite sign from the other cell. This imbalance forms a charge build-up and the excess carriers will relax to the ground state eventually. Therefore, the overall current will be limited by the lowest amount of generated free carriers of the subcells. The increase in efficiency should come from an increased open-circuit voltage, in the perfect case the open-circuit voltage will be the sum of the  $V_{oc}$ 's of the separate subcells. The recombination center should allow efficient recombination of electrons flowing out of the acceptor of the first cell and holes flowing out of the donor of the second cell without

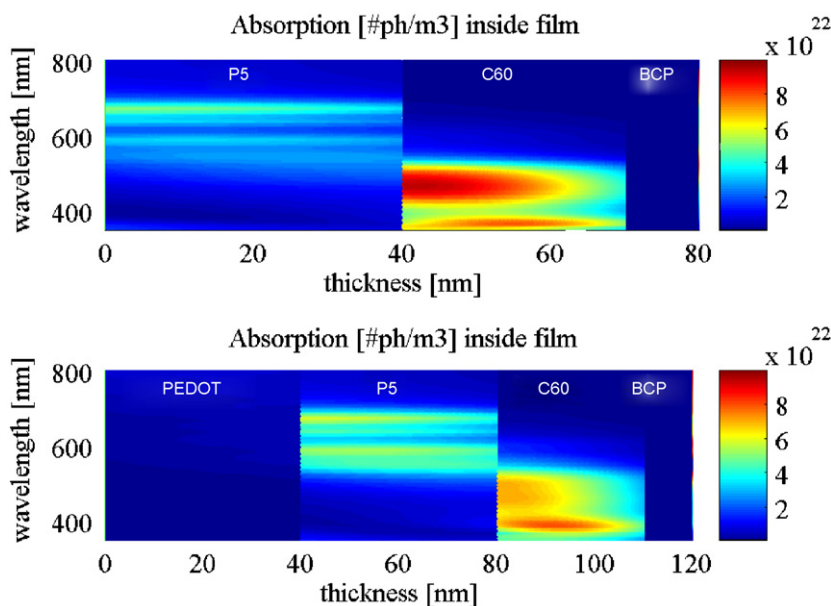


Fig. 4. Absorbed photons (color) as a function of the wavelength ( $y$ -axis) and the position inside the organic layers ( $x$ -axis) due to optical interference. The incident light is broadband normalized light, coming in from the left. The upper figure is a simulation carried out for a layer structure of ITO (not shown)/40 nm pentacene (P5)/30 nm C<sub>60</sub>/10 nm BCP/70 nm Al (not shown), the lower figure is a simulation carried out for a layer structure of ITO (not shown)/40 nm PEDOT:PSS/40 nm pentacene (P5)/30 nm C<sub>60</sub>/10 nm BCP/70 nm Al (not shown).

introducing an energy loss. Experimentally, stacked cells with a thin metal layer as recombination center show a double open-circuit voltage compared to single cells [8,9].

The schematic energy diagram of a stacked solar cell is shown in Fig. 5. An electron traveling from the acceptor to the mid-contact will lose energy equal to the difference between the LUMO of the acceptor ( $LUMO_A$ ) and the workfunction of the metal used as mid-contact. At the same time, holes from the donor lose energy equal to the difference between the HOMO of the donor ( $HOMO_D$ ) and the workfunction of the mid-contact. The total loss would be an energy equal to  $HOMO_D - LUMO_A$ , but this is not seen experimentally. A possible explanation of the experiments is the formation of dipoles between the organic materials and the mid-contact [21]. This decreases the energy loss at the contact.

We propose another mechanism for the experimental observed increase of open-circuit voltage for the stacked cells compared to the single cell. This mechanism is based on the work of Barker et al. [22] and uses the assumption of important diffusion currents in the layers. As the recombination center accepts both electrons and holes, the carriers will recombine very fast. Any inequality of carriers would produce an attractive force for the carriers of the other sign toward the recombination zone. The steady state carrier densities at the mid-contact are low. At the donor–acceptor interface, carriers are generated and the steady state carrier densities are high. This density difference introduces a diffusion current from the donor–acceptor interface towards the mid-contact. At  $V_{oc}$  this current should be balanced by an equal drift current in the opposite direction, as such decreasing the overall current to zero. This drift current must be produced by an electrical field, or a certain band-bending in the energy levels. The band-bending will be equal to the energy loss at the mid-contact

( $HOMO_D - LUMO_A$ ), producing an increased  $V_{oc}$  for tandem structures, doubling the  $V_{oc}$  when currents of the two subcells are matched.

For the stacked devices the structure of the single cell (40 nm pentacene/30 nm  $C_{60}$ ) is repeated twice, with a metal layer in between the two cells. Different thin metal layers ( $\pm 5 \text{ \AA}$ ) are used as recombination centers. These metals are aluminum (Al, cell T1 on PEDOT:PSS and T2 on ITO), gold (Au, cell T3 on PEDOT:PSS and T4 on ITO) and silver (Ag, cell T5 on PEDOT:PSS and T6 on ITO). The cells are capped with 10 nm BCP and 70 nm aluminum. The complete cell is made without breaking the vacuum. The results are shown in Fig. 6 ( $I$ – $V$  characteristics) and in Table 1 (cell performance parameters).

Stacked cells with aluminum as mid-contact produce S-shaped diode characteristics. The  $V_{oc}$  is lower than the  $V_{oc}$  of the single cell for both the cells with (0.22 vs. 0.29 V)

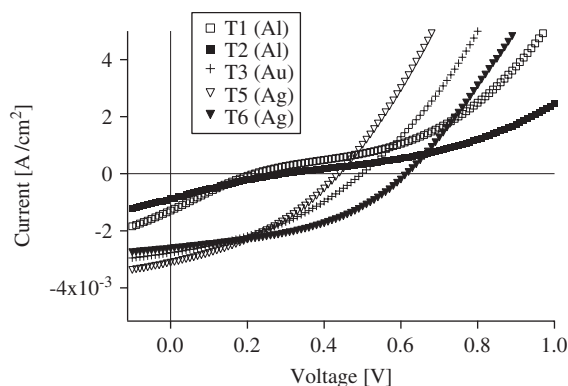


Fig. 6.  $I$ – $V$  curves of stacked cells. The structures are stacked planar heterojunction cells with (T1, T3, T5) and without (T2, T6) PEDOT:PSS layer on top of the ITO. Further layer structure: 40 nm pentacene/30 nm  $C_{60}$ /0.5 nm metal layer/40 nm pentacene/30 nm  $C_{60}$ /10 nm BCP/70 nm Al. The metal layer is aluminum (T1 and T2), gold (T3 and T4) or silver (T5 and T6).

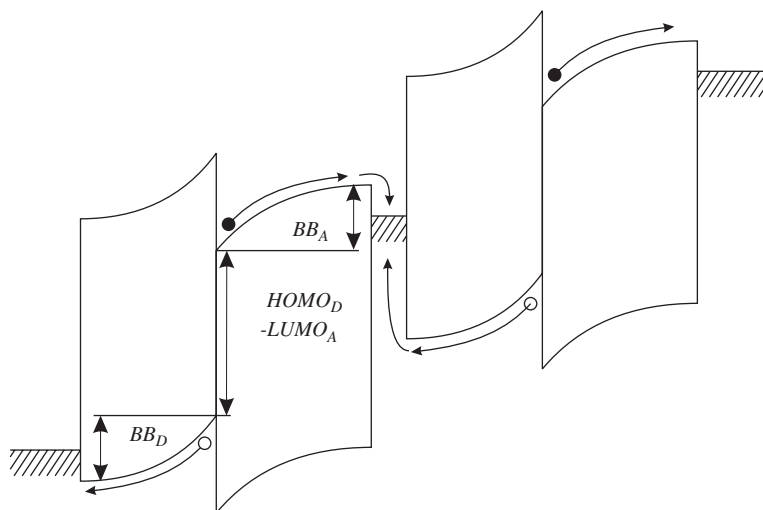


Fig. 5. Schematic energy level diagram for a stacked organic solar cell around open-circuit voltage.  $BB_D$  and  $BB_A$  are band-bendings inside the organic films due to diffusion current.

Table 1  
Overview of solar cell performance parameters for single and stacked cells

| Cell | $V_{oc}$ (V) | $I_{sc}$ (mA/cm <sup>2</sup> ) | FF (%) | $\eta$ (%) |
|------|--------------|--------------------------------|--------|------------|
| S1   | 0.29         | 6.7                            | 51     | 0.55       |
| S2   | 0.35         | 5.6                            | 53     | 0.58       |
| T1   | 0.22         | 1.29                           | 23     | 0.03       |
| T2   | 0.3          | 0.65                           | 21     | 0.03       |
| T3   | 0.52         | 2.34                           | 37     | 0.25       |
| T4   | 0            | 0                              | 0      | 0          |
| T5   | 0.45         | 3                              | 35     | 0.26       |
| T6   | 0.62         | 2.6                            | 46     | 0.41       |

S1 and S2 are single planar heterojunction cells with and without 40 nm PEDOT:PSS, respectively, with layer structure as mentioned in Fig. 1. The other cells are stacked planar heterojunction cells with layer structure as mentioned in Fig. 6.

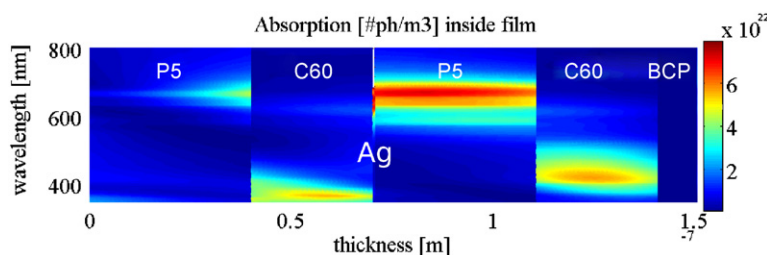


Fig. 7. Absorbed photons (color) as a function of the wavelength ( $y$ -axis) and position inside the organic layer structure ( $x$ -axis) due to optical interference. The incident light is broadband normalized light, coming in from the left. This simulation has been carried out for a stacked cell with layer structure ITO (not shown)/40 nm pentacene/30 nm  $C_{60}$ /0.5 nm Ag/40 nm pentacene/30 nm  $C_{60}$ /10 nm BCP/70 nm Al (not shown).

and without (0.3 vs. 0.35 V) PEDOT:PSS. The S-shaped  $I$ - $V$  characteristic can be attributed to a barrier for extraction inside the solar cell. We suspect oxidation of the aluminum causing poor recombination. As a consequence carriers pile up close to the mid-contact aluminum, limiting the open-circuit voltage and overall cell behavior.

If different metals are used as recombination center in between the two cells, better cell performance is observed. The  $V_{oc}$  increases, effectively showing a double open-circuit voltage compared to a single cells when using a silver mid-contact and cells made on ITO substrates. Using the same substrates without PEDOT:PSS and gold as mid-contact failed since all the cells where shunted. This could be caused by diffusion of gold inside the organic layers and the different morphology of pentacene grown on ITO (see Fig. 2). Overall fill factors are still lower than the fill factors of a single cell, so further optimization of the mid-contact is necessary. A limiting factor for high efficiencies is the low short-circuit current. As no optical optimization has been done, this could drastically improve the current. Fig. 7 shows a simulation of the amount of absorbed photons inside the stacked cell with silver as mid-contact (cell T6). The amount of absorbed photons in the first cell is lower than the amount of absorbed photons of the second cell. The overall current will be limited by the lowest current of the separate cells, in this case the first cell. By using a different layer structure the interference patterns should be tuned for equal and maximum absorption in both subcells.

#### 4. Conclusion

We have studied different metals as efficient recombination centers for use in stacked organic solar cells based on pentacene and  $C_{60}$ . The open-circuit voltage and short-circuit current of single cells differs with and without PEDOT:PSS. We discuss two possibilities for this difference. First a different morphology is observed for pentacene thin films grown on PEDOT:PSS and on ITO. A second possible change is the optical interference which is important for the amount of absorbed photons inside the layer structure. In a next step stacked cells with the same active layer materials were fabricated. Aluminum is demonstrated to be an inefficient recombination center, while both gold and silver show promising results, increasing the open-circuit voltage. We propose a model based on diffusion of carriers from the donor-acceptor interface to the recombination center as explanation for the working principle of the stacked solar cell. Due to this diffusion current a higher voltage is needed to get to the open-circuit point. In the end, cells without PEDOT:PSS and with silver as recombination center show a doubling of the open-circuit voltage compared to single cells. Further optical optimization of the layer structure and using bulk heterojunction layers should increase the efficiency.

#### Acknowledgments

We thank the European project MolyCell (Contract no. 502783) for the financial support.

**References**

- [1] C.W. Tang, *Appl. Phys. Lett.* 48 (2) (1986) 183.
- [2] N.S. Sariciftci, L. Smilowitz, A.J. Heeger, F. Wudl, *Science* 258 (1992) 1474.
- [3] G. Yu, J. Gao, J.C. Hummelen, F. Wudl, A.J. Heeger, *Science* 270 (1995) 1789.
- [4] P. Peumans, S. Uchida, S.R. Forrest, *Nature* 425 (2003) 158.
- [5] G. Li, V. Shrotriya, J. Huang, Y. Yao, T. Moriarty, K. Emery, Y. Yang, *Nat. Mat.* 4 (2005) 864.
- [6] P. Vanlaeke, A. Swinnen, I. Haeldermans, G. Vanhoyland, T. Aernouts, D. Cheyns, C. Deibel, J. D'Haen, P. Heremans, J. Poortmans, J.V. Manca, *Sol. Energy Mater. Sol. Cells* 90 (14) (2006) 2150.
- [7] J. Xue, S. Uchida, B.P. Rand, S.R. Forrest, *Appl. Phys. Lett.* 84 (16) (2004) 3013.
- [8] M. Hiramoto, M. Suezaki, M. Yokoyama, *Chem. Lett.* 19 (3) (1990) 327.
- [9] A. Yakimov, S.R. Forrest, *Appl. Phys. Lett.* 80 (9) (2002) 1667.
- [10] J. Dreschel, B. Männig, F. Kozlowski, M. Pfeiffer, K. Leo, H. Hoppe, *Appl. Phys. Lett.* 86 (2005) 244102.
- [11] S. Yoo, B. Domercq, B. Kippelen, *Appl. Phys. Lett.* 85 (22) (2004) 5427.
- [12] A.C. Mayer, M.T. Lloyd, D.J. Herman, T.G. Gasen, G.G. Malliaras, *Appl. Phys. Lett.* 85 (25) (2004) 6272.
- [13] S. Kobayashi, T. Takenobu, S. Mori, A. Fujiwara, Y. Iwasa, *Appl. Phys. Lett.* 82 (25) (2003) 4581.
- [14] T.W. Kelley, P.F. Baude, C. Gerlach, D.E. Ender, D. Muires, M.A. Haase, D.E. Vogel, S.E. Theiss, *Chem. Mater.* 16 (23) (2004) 4413.
- [15] D.F. O'Brien, M.A. Baldo, M.E. Thompson, S.R. Forrest, *Appl. Phys. Lett.* 74 (3) (1999) 442.
- [16] P. Peumans, S.R. Forrest, *Appl. Phys. Lett.* 79 (1) (2001) 126.
- [17] L.A.A. Pettersson, L.S. Roman, O. Inganäs, *J. Appl. Phys.* 86 (1) (1999) 487.
- [18] P. Peumans, A. Yakimov, S.R. Forrest, *J. Appl. Phys.* 93 (7) (2003) 3693.
- [19] H. Hoppe, N. Arnold, N.S. Sariciftci, D. Meissner, *Sol. Energy Mater. Sol. Cells* 80 (1) (2003) 105.
- [20] R.M.A. Azzam, N.M. Bashara, *Ellipsometry and Polarized Light*, Elsevier, Amsterdam, 1987.
- [21] B. Maennig, J. Drechsel, D. Gebeyehu, P. Simon, F. Kozlowski, A. Werner, F. Li, S. Grundmann, S. Sonntag, M. Koch, K. Leo, M. Pfeiffer, H. Hoppe, D. Meissner, N. Sariciftci, I. Riedel, V. Dyakonov, J. Parisi, *Appl. Phys. A* 79 (2004) 1.
- [22] J.A. Barker, C.M. Ramsdale, N.C. Greenham, *Phys. Rev. B* 67 (2003) 07520.